Silica, carbon and boron nitride monoliths with hierarchical porosity prepared by spark plasma sintering process

Philippe Dibandjo, Laurence Bois, Claude Estournès, Bernard Durand, Philippe Miele

Silica, carbon and boron nitride monoliths with hierarchical porosity prepared by spark plasma sintering process

Philippe Dibandjo [a,*], Laurence Bois [a], Claude Estournes [b,c], Bernard Durand [b], Philippe Miele [a,*]

[a] *LMI, UMR CNRS 5615, Université Claude Bernard-Lyon 1, 43 bvd du 11 novembre 1918, 69622 Villeurbanne Cedex, France*
[b] *CIRIMAT, UMR 5085, UPS, 118, route de Narbonne 31062 Toulouse Cedex 9, France*
[c] *Plateforme Nationale de Frittage Flash (PNF2) du CNRS, MHT, Université Paul Sabatier 118, route de Narbonne 31062 Toulouse Cedex 9, France*

Abstract

Silica SBA-15, carbon CMK-3, boron nitride (BN), the latter synthesized from the first two compounds as templates, are mesoporous materials in the form of powders. They have a high specific surface area and an important mesoporous volume. The porosity is organized with the hexagonal symmetric space group p6mm. For selected applications, it could be interesting to preserve these characteristics with materials in a well-defined shape at a macroscopic scale (few millimeters to centimeter). Spark plasma sintering (SPS) is a well-known technique which allows to prepare monoliths with relatively mild conditions. The SPS technique has been used on these mesoporous powders without charge or with a uniaxial charge and at temperatures of 600 °C, 800 °C for silica, 1100 °C, 1300 °C for carbon and 1600 °C, 1700 °C for boron nitride during 1–5 min. The nitrogen adsorption/desorption isotherms reveal that the obtained monoliths present high specific surface area (300–500 m^2/g) and important mesoporous volume. The coexistence of interconnected mesoporosity and macroporosity (with volume's close value) was observed by SEM and TEM, while the XRD and TEM characterization show that the mesoporosity organization is partially preserved.

Keywords: Sintering; Silica; Carbon; Boron nitride (BN); Mesoporosity; Monoliths

1. Introduction

Mesoporous materials have been widespread used as sorbents, filters, catalyst supports, electrode materials, sensors, electrochemical double-layer capacitors, chromatographic materials, hydrogen storage systems, and in many others applications [1–3]. For many of these applications, hierarchically porous materials that have well-defined macropores and interconnected meso- and/or micropores have great interest, since they are expected to have enhanced properties compared to monomodal porous materials [4]. Hierarchical porosity enables high solid–fluid exchange associated with small pores, combined with the high flow rates associated with large pores.

Synthesis of mesoporous materials is a subject of intensive research since the past decade, as documented in various reviews [5–8]. Most of these mesoporous materials are based on silica, oxides and carbon. Recently, we have reported for the first time the synthesis of mesoporous boron nitride with ordered mesoporosity by the nanocasting pathway [9,10], whereas nanostructured BN has also been prepared via a self-assembly process [11]. Most of these materials are obtained in powder form, which limits their potential application, due to a difficult recovery, high-pressure drop and dust problem as well [12]. It could therefore be interesting to develop mechanically stable and self-supporting monolithic mesoporous materials.

* Corresponding authors.
E-mail addresses: philippe.dibandjo@ing.unitn.it (P. Dibandjo), laurence.bois@univ-lyon1.fr (L. Bois).

doi:10.1016/j.micromeso.2007.07.036

The spark plasma sintering (SPS) is a very powerful technique that allows the elaboration of resistant pellets at lower temperatures in comparison with classic sintering methods [13]. It allows very fast heating and cooling rates as well as very short holding times. It is more and more often put into practice to solve problems even in the industrial field. The advantages of this technique comes from the very high sintering speed, which avoids the particles enlargement and which limits the particles surface reactions.

In the present study, we have sintered powders of silica SBA-15 [6], carbon CMK-3 [8] and mesoporous boron nitride (BN) [9] by the SPS method. The starting powders have high specific surface area, important mesoporous volume organized in an hexagonal system. Textural properties of the starting powders are mostly preserved in the resulting monoliths which offers great outlooks.

2. Experimental section

2.1. Powders preparation

The ordered mesoporous SBA-15 silica has been prepared following the procedure reported by Zhao et al. [14]. Hydrolysis and condensation of TEOS is performed in presence of a block copolymer Pluronic P123 in acidic conditions. A calcination of the composite block copolymer-silica (at 500 °C in air) permits the elaboration of the mesoporous silica SBA-15.

The synthesis of the CMK-3 carbon template is performed using the SBA-15 mesoporous silica [14] as the template and sucrose as carbon source, following the synthesis procedure reported by Jun et al. [8] The high specific surface area is associated with an important volume of cylindrical geometry mesopores with narrow pore size distribution organized in the hexagonal space group p6mm. The presence of micropores connected to mesopores does not only contribute to the specific surface area, but also plays an important part in the nanocasting process [15].

The synthesis of ordered mesoporous boron nitride is performed by using a nanocasting process of a mesoporous CMK-3 carbon with a borazinic precursor. The borazinic precursor, tri(methylamino)borazine, $(CH_3NH)_3B_3N_3H_3$ (MAB), has been converted to boron nitride (BN) inside the mesopores of a CMK-3 mesoporous carbon template following the procedure described by Dibandjo et al. [9].

After characterization, the different synthesised powders have been sintered inside the ''SPS'' instrument.

2.2. SPS sintering

The sintering process has been performed with a ''SPS 2080 SUMIMOTO'' instrument (CIRIMAT, Toulouse, France), either without or with a charge of 25 MPa applied immediately at the beginning of the experience or during heating. The usual heating rate used in all the experiments is 100 °C min^{-1} and the maximum temperature is 600 or 800 °C, for the silica (samples SM1, SM2, SM3), 1100 or 1300 °C for carbon (samples CM1,CM2) and 1600 or 1700 °C for boron nitride (samples BM1, BM2). In the case of carbon and boron nitride, the experience has been carried out in a nitrogen atmosphere. All the obtained monoliths have a cylindrical form with a diameter of 8 mm and height of few mm (3–5 mm).

2.3. Characterization

Beside a chemical analysis, structural and morphological characterizations of the samples have also been carried out.

Powder X-ray diffraction (XRD) patterns have been recorded on a Xpert PANanalytical diffractometer equipped with a monochromator, using CuKα radiation. Small-angle X-ray diffraction patterns have been acquired between 0.5° and 5° and a time of 200 s per step.

Nitrogen adsorption/desorption isotherms have been measured on a Sorptomatic 1900 analyzer (Fisons). Before the adsorption measurements, the samples have been outgassed for 4 h at 150 °C in the degas port of the adsorption analyzer. The BET specific surface area has been calculated from the nitrogen adsorption data in the relative pressure range from 0.05 to 0.3. The pore size distribution has been analyzed with N_2 adsorption branch, following the BJH (Barret–Joyner–Halenda) algorithm. The mesoporous volume has been calculated between a relative pressure of 0.4 and 0.95.

The TEM images have been taken with a TOPCON EM002B transmission electron microscope operating at 200 kV. Samples for the TEM measurement have been supported on a carbon-coated grid. The SEM images have been recorded with a HITASHI S800 scanning electron microscope operating at 15 kV.

The ACCUPYC 1330 MICROMERITICS apparatus has been used to obtain the helium density of the different sintered samples.

3. Results

The integrated process for producing stable hierarchical monoliths involves three steps, namely (i) the synthesis of mesoporous powders, (ii) the instrument chamber filling with the mesoporous powders, and (iii) the rapid heating of the powders at the desired temperature. In some cases, a pressure is simultaneously applied.

3.1. Porous volume determination

Similarly to the results obtained with the starting powders, the N_2 adsorption–desorption isotherms of the monoliths are characteristic of mesoporous materials (type IV) [16] (Fig. 1). The silica monoliths isotherms present a hysteresis loop of H1 type whereas those of carbon and BN monoliths show hysteresis loop of H2 type [17]. The mean

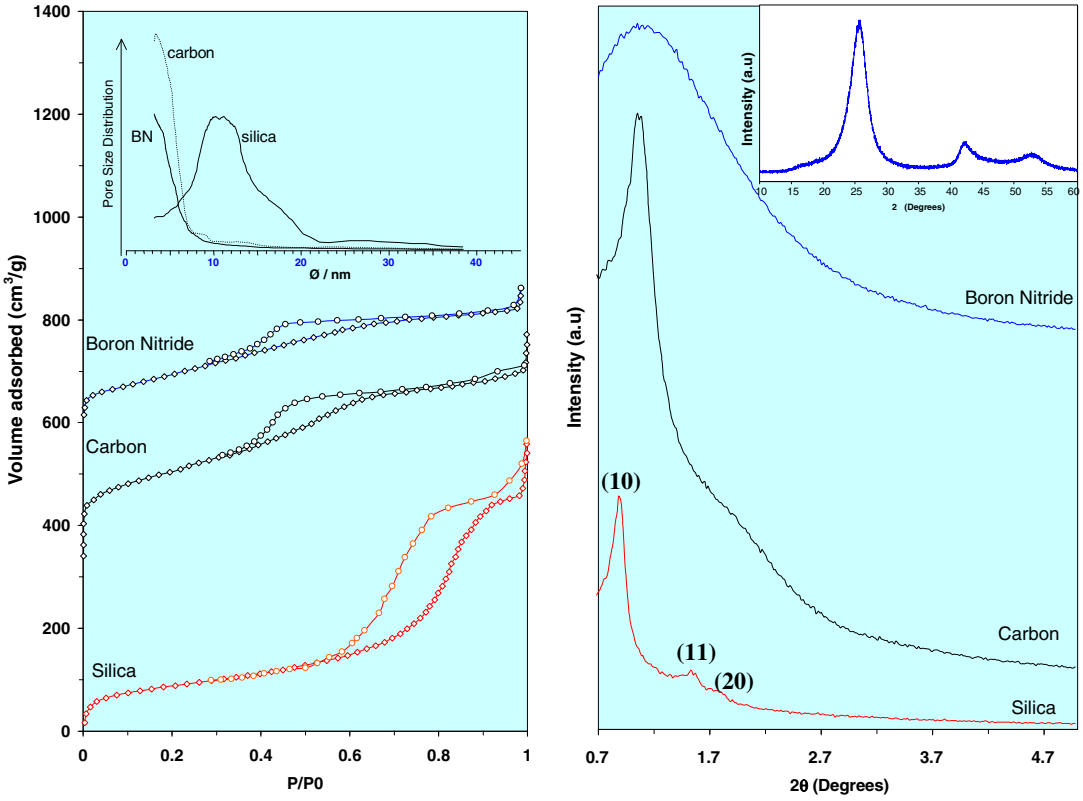

Fig. 1. Nitrogen sorption isotherms, pore diameter distribution curves and X-ray diffraction patterns of silica, carbon, and boron nitride monoliths.

pore diameter of mesopores of the powders is retained in the monoliths (Fig. 1). The size distribution is still narrow. In contrast, the monoliths specific surface areas decrease after the sintering process but still have high values. The hysteresis loop of the different monoliths around a relative pressure $P/P_0 = 0.9$, can be attributed to the formation of intergranular mesopores. The macroporous volume is formed by a partial coalescence of the particles. The structure consolidation is the result of the intensive Joule effect at the contact points between neighbouring particles. In order to estimate the macroporous volume (V_{macro}) (Table 1), the following relation has been used:

$$V_{\text{macro}} = 1/\rho_{\text{a}} - 1/\rho_{\text{h}} - V_{\text{meso}}$$

in which ρ_{a} is the apparent bulk density and, ρ_{h} is the Helium bulk density (Table 2) and V_{meso} the mesoporous volume, all are measured values, except for ρ_{h} values of BM monoliths. This relation is valid assuming that the microporous volume can be neglected.

For the SM monoliths, the macroporous volume is lower than the mesoporous volume. The mesoporous volume decreases when the temperature increases or when the pressure is applied. For the CM and BM monoliths, macroporous volume is higher than the mesoporous volume, but also decreases with an increase of the sintering temperature.

The evolution of the specific surface area and mesoporous volume of the different monoliths suggest that the deformation of the contact points of the hexagonal particles results in only a local elimination of pores.

3.2. Porosity organization

The silica (SM), carbon (CM) and boron nitride (BM) monoliths as well as the starting powders have been characterized by XRD. The small angles XRD patterns (Fig. 1) of the SM monoliths show well-resolved reflections similar to those of the starting SBA-15 powder, which can be indexed as (10), (11) and (20) in 2D hexagonal symmetry. The (10) interreticular distance of SM monoliths is of 10.0 nm. For the CM monoliths, the XRD pattern has a reflection peak having a d spacing of 8.33 nm corresponding to (10) reflection, indicating that the pore structure is uniform and ordered. The BM monoliths present a broad peak around 8 nm that can be explained by a short range order of the pores. On the XRD pattern, hexagonal boron nitride crystallization is starting, with the reflections (002), (10) and (004) at $2\theta = 26°$ 43° and 54°.

The fully porous nature of the monoliths is evidenced by the TEM images in which the homogeneously distributed textural porosity can be clearly observed. The TEM images of the SM and CM materials provide additional structural information and confirm the structure organization (Fig. 2a and b). On the image of SM monolith (Fig. 2a), strongly contrasted parallel channels are distant of 11.1 nm. Between these channels, we can also distinguish

Table 1
Textural characteristics for the silica, carbon, boron nitride powders and SM, CM, BM monoliths determinated from nitrogen sorption measurements

Sample	Total porous volume (cm^3/g)	Mesoporous volume (cm^3/g)	Macroporous volume (cm^3/g)	S_{BET} (m^2/g)	Pore diameter (mean) (nm)	Pore diameter (max) (nm)
Silica	1.06	1.02	–	450	11.25	10.4
SM1	1.48	0.84	0.64	380	11.8	12.2
SM2	1.03	0.67	0.36	323	11.3	12.2
SM3	1.02	0.64	0.38	298	10.9	10.2
Carbon		0.69	–	770	4.7	4.3
CM1	1.16	0.50	0.66	706	4.6	4.1
CM2	0.91	0.42	0.49	743	4.6	4.2
Boron nitride	0.73	0.22	–	1100	4.1	3.2
BM1	0.33	0.20	0.63	428	4.3	3.2
BM2	0.26	0.17	0.37	274	4.9	3.4

Total porous volume: Total pore volume at $P/P_0 = 0.95$. Mesoporous volume: Calculated according to BJH (adsorption branch between for $0.4 < P/P_0 < 0.95$). Macroporous volume: calculated according to $V_{macro} = 1/\rho_a - 1/\rho_h - V_{meso}$ S_{BET}: specific surface area according to BET. Pore diameter (mean): mean of pore diameter according to BJH (adsorption branch). Pore diameter (max): max of pore diameter according to BJH (adsorption branch).

Table 2
Temperature and applied pressure

Sample	Temperature (°C)	Applied pressure (MPa)	Helium density (g/cm^3)	Apparent density (g/cm^3)	Linear shrinkage (%)
SM1	600	0	2.234	0.520	–
SM2	600	25	2.374	0.691	33.5
SM3	800	0	2.306	0.687	31.3
CM1	1100	25	2.104	0.613	19.3
CM2	1300	25	2.051	0.716	32.9
BM1	1600	0	2.18	0.786	
BM2	1700	2	2.18	1.015	41.7

Total shrinkage, apparent and measured bulk densities.
Temperature: Maximal temperature during SPS process. Applied pressure: Pressure used during SPS process. Helium density: Measured with ACCUPYC 1330 MICROMERITICS apparatus, except for BM samples. Apparent density: Calculated from geometric consideration. Linear shrinkage (%): shrinkage (mm)/[shrinkage (mm) + final thickness (mm)].

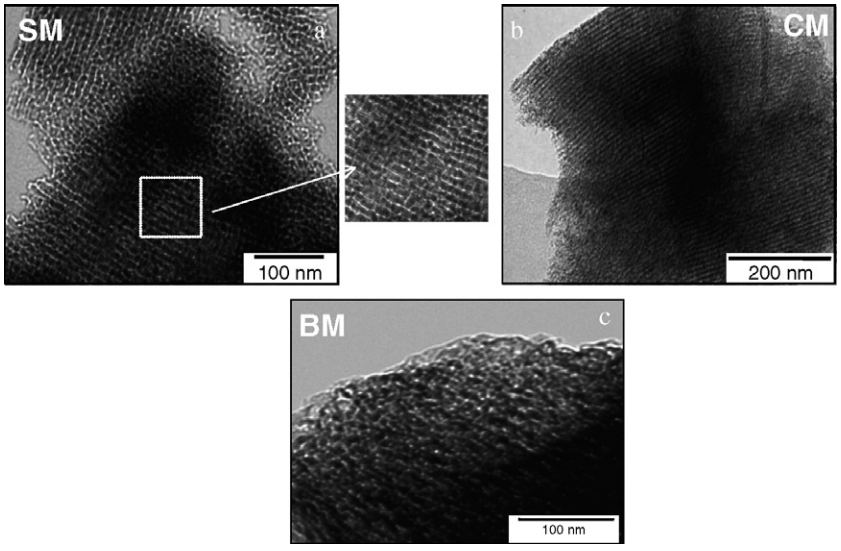

Fig. 2. TEM images of (a) SM1, (b) CM1 and (c) BM2 monoliths.

isolated secondary channels distant approximately from 2.7 nm. The organization of the pores repartition is also confirmed by many others images while a variation of the distance between the main channels (9–11 nm) can be observed. For the CM monoliths (Fig. 2b), the parallel channels are always observed with a distance of 8.4 nm in

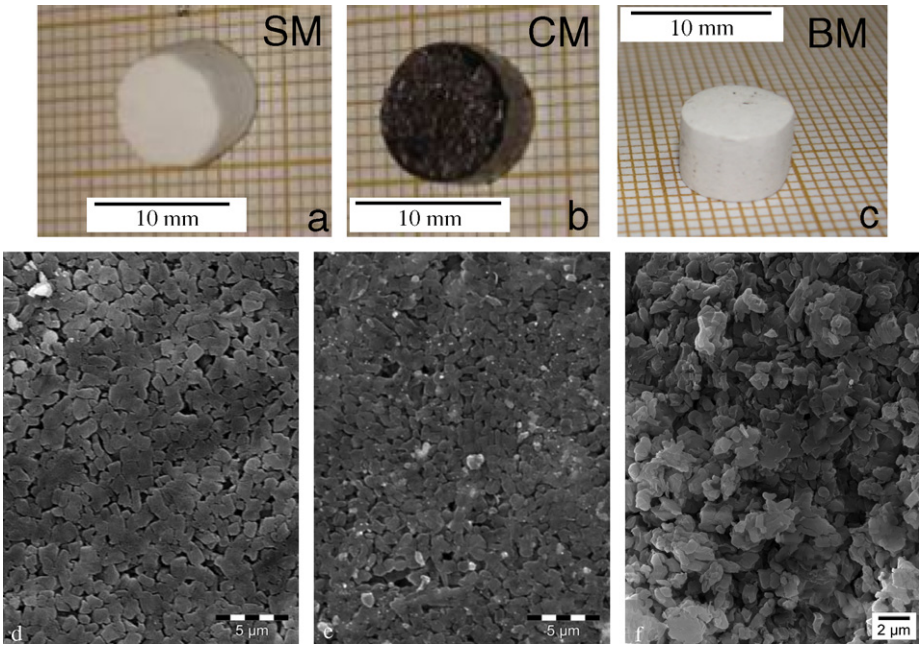

Fig. 3. Representative photos of the monoliths studied : (a) silica, (b) carbon, (c) boron nitride and SEM images of (d) silica SM1, (e) carbon CM1 and (f) boron nitride BM2 monoliths.

good agreement with the (10) d spacing value obtained by XRD analysis. The SM and CM structures are highly interconnected and homogeneous in nature, which are also reflected by the high mechanical stability of the monoliths. The BM monoliths (Fig. 2c), show a porous structure without order. This can be explained by the low ordered in the porosity of the starting powder.

Fig. 3 shows the representative photos and SEM images of the different monoliths. The images confirm the existence of a macroporosity with pores of micrometric size. In Fig. 3a, mesopores can also be distinguished.

4. Discussion

The properties of the SM, CM, BM monoliths can be described by comparison with those of the monoliths obtained by conventional natural sintering at the same temperatures. In the latter case, it is for instance necessary to compact the silica powder sufficiently in order to carry out the cohesion of the monolith that causes a crushing of the mesoporous channels [18–20]. Under similar sintering conditions, for carbon and boron nitride, it is not even possible to obtain a monolith.

The properties of monoliths sintered by the SPS process are related to the advantages of this technique which allows the surface reactions by avoiding the enlargement of the particle, more especially due to the fact that the experiment proceeds at low temperature. Problems with shrinkage and cracking that often plague solution-based methods are insignificant, and it is possible to manufacture large objects in short time.

When the temperature remains moderate and with the value of constraint used, the material mesoporosity is preserved and the partial coalescence of the particles generates the macroporous volume. The collapse of the microporosity with the profit of mesoporosity causes a light increase of the pores diameter in accordance with the observations carried out on the thermal treatment of mesoporous compounds [21].

The SPS technique makes possible to maintain the mesopores organization without important modification. This result is in good agreement with the studies concerning the nanostructure evolution of mesoporous silica and carbons powders with temperature. For the silica powders, the stability of mesopores remains up to 1000 °C and depends on the thickness of the walls [8,18]. For the mesoporous CMK-3 carbon, the nanostructure organization collapses when the crystallographic structure of CMK-3 carbon changes from the turbostatic into the graphitic one, and this phenomenon is observed around 1600 °C [22]. In the case of mesoporous boron nitride, the first studies describing the stability of this ceramic has shown that the mesoporosity is preserved up to 1700 °C, which could be correlated to the hexagonal boron nitride crystallization which is beginning at this temperature [21]. By contrast, the SPS technique allows to obtain a hierarchical boron nitride at 1700 °C with an hexagonal structure. Thus, this is the first time to our knowledge that hexagonal boron nitride displaying both a high degree of crystallization and an organized mesoporosity could be obtained at this temperature which is undoubtedly a result of primary importance.

5. Conclusion

The « SPS » sintering method makes possible to obtain boron nitride, carbon and silica monoliths combining

mesoporosity (between 0.2 and 0.8 cm^3/g) and macroporosity (between 0.6 and 0.8 cm^3/g) with a density corresponding to 25 or 30% of the theoretical density of the compound. The mechanical stability of such hierarchical monoliths opens up many large-scale applications for advanced materials. In comparison with the starting powders, the mesoporous volume of the resulting monoliths slightly decreases, but still preserves a high value (0.8 cm^3/g for silica, 0.5 cm^3/g for carbon and 0.2 cm^3/g for boron nitride). The specific surface area of the different monoliths decreases with the increase of the temperature of sintering (300–500 m^2/g). Finally, the mesopores initial organization in a p6mm space group is little disturbed by this type of sintering, especially for carbon materials.

The success of the preparation of carbon and boron nitride mesoporous monoliths, which are typical covalent compounds, more difficult to sinter than silica encourages us to extend the sintering method to others type of mesoporous non-oxide materials. Further works are currently in progress in this area around binary, ternary and quaternary compositions.

Acknowledgment

We acknowledge Prof. Jean-Pierre Deloume (IRCELYON, UMR CNRS 5256 Université Claude Bernard-Lyon I) for giving us an access to the measurements of the helium density.

References

[1] M. Davis, Nature 417 (2002) 813.
[2] F. Schuth, W. Schmidt, Adv. Eng. Mater. 4–5 (2002) 269–279.
[3] R. Ryoo, S.H. Joo, M. Kruk, M. Jaroniec, Adv. Mater. 13 (2001) 677–681.
[4] R. Backov, Soft Matter 2 (2006) 452–464.
[5] J.S. Beck, J.C. Vartuli, W.J. Roth, M.E. Leonowicz, C.T. Kresge, K.D. Schmitt, C.T.W. Chu, D.H. Olson, E.W. Sheppard, et al., J. Am. Chem. Soc. 114 (1992) 10834–10843.
[6] D. Zhao, P. Yang, Q. Huo, B.F. Chmelka, G.D. Stucky, Curr. Opin. Solid State Mater. Sci. 3 (1998) 111–112.
[7] J.A.A. Soler-Illia Galo, L. Crepaldi Eduardo, D. Grosso, C. Sanchez, Curr. Opin. Colloid. Interface Sci. 8, 1 (2003) 109–126.
[8] S. Jun, S.H. Joo, R. Ryoo, M. Kruk, M. Jaroniec, Z. Liu, T. Ohsuna, O. Terasaki, J. Am. Chem. Soc. 122 (2000) 10712–10723.
[9] P. Dibandjo, L. Bois, F. Chassagneux, D. Cornu, B. Toury, F. Babonneau, P. Miele, Adv. Mater. 17 (2005) 571.
[10] P. Dibandjo, F. Chassagneux, L. Bois, C. Sigala, P. Miele, J. Mater. Chem. 15 (2005) 1917–1923.
[11] P.R.L. Malenfant, J. Wan, S.T. Taylor, M. Manoharan, Nature Nanotech. 2 (2007) 43–46.
[12] A. Galarneau, J. Lapichella, D. Bruel, F. Fajula, Z. Bayram-Hahn, K. Unger, G. Puy, C. Demesmay, J.L. Rocca, J. Sep. Sci. 29 (6) (2006) 844–855.
[13] M. Nygren, Z. Shen, Solid State Sci. 5 (2003) 125–131.
[14] D. Zhao, J. Feng, Q. Huo, N. Melosh, G.H. Fredrickson, B.F. Chemla, G.D. Stucky, Science 279 (1998) 542–548.
[15] R. Ryoo, C.H. Ko, M. Kruk, V. Antochshuk, M. Jaroniec, J. Phys. Chem. B 104 (2000) 11465–11471.
[16] J. Rouquerol, D. Avnir, CW. Fairbridge, D.H. Everett, J.H. Haynes, N. Pernicone, J.D.F. Ramsay, K.S.W. Sing, K.K. Unger, Pure Appl. Chem. 66 (1994) 1739–1758.
[17] K.S.W. Sing, D.H. Everett, J.H. Haynes, R.A.W. Hall, L. Moscou, R.A. Pierotti, J. Rouquerol, T. Siemienewska, Pure Appl. Chem. 57 (1985) 603–609.
[18] A. Galarneau, D. Desplantier-Giscard, F. Di Renzo, F. Fajula, Catal. Today 68 (2001) 191–200.
[19] M. Hartmann, A. Vinu, Langmuir 18 (2002) 8010–8016.
[20] J.J. Chiu, D.J. Pine, S.T. Bishop, B.F. Chmelka, J. Catal. 221 (2004) 400–412.
[21] P. Dibandjo, L. Bois, F. Chassagneux, P. Miele, J. Eur. Ceram. Soc. 27 (1) (2007) 313–317.
[22] H. Darmstadt, C. Roy, S. Kaliaguine, S.H. Joo, R. Ryoo, Micropor. Mesopor. Mat. 60 (2003) 139–149.